1660 *Inorg. Chem.* **1994,** *33,* 1660–1665

Reactivity of $Pd(PH_3)_2$ for Oxidative Additions of the Si–X σ-Bonds (X = H, C, Si). An ab Initio MO/MP4 Study

Shigeyoshi Sakaki,* Masahiro Ogawa, Yasuo Musashi, and Toru Arai

Department of Applied Chemistry, Faculty of Engineering, Kumamoto University,
Kurokami, Kumamoto 860, Japan

Received July 2, 1993[⊗]

Oxidative addition of the Si–X σ-bond (X = H, C, Si) to $Pd(PH_3)_2$ is theoretically investigated with the ab initio MO/MP4 method. The activation barrier (E_a) and the energy of reaction (ΔE) estimated at the MP4(SDQ) level are 13.5 and 18.1 (19.6 and –46.4) kcal/mol, respectively, for the Si–Si oxidative addition, 21.5 and 8.1 (29.5 and –14.1) kcal/mol, respectively, for the Si–C oxidative addition, and about 2 and –8.1 (1.8 and –31.1) kcal/mol for the Si–H oxidative addition, where in parentheses are given E_a and ΔE of the reaction with $Pt(PH_3)_2$ (from our previous work published in *J. Am. Chem. Soc.* **1993**, *115*, 2373) and a negative ΔE value represents exothermicity. Although Si–X oxidative addition to $Pd(PH_3)_2$ is much less exothermic (or much more endothermic) than the corresponding oxidative addition to $Pt(PH_3)_2$, the E_a value of the former is slightly smaller than (or similar to) that of the latter, suggesting that the Si–X oxidative addition to $Pd(PH_3)_2$ as well as its oxidative addition to $Pt(PH_3)_2$ easily proceeds in spite of the smaller exothermicity. The smaller exothermicity (or larger endothermicity) of the Si–X oxidative addition to $Pd(PH_3)_2$ is because the Pd–X bond is weaker than the Pt–X bond. The reason for the rather small E_a value is that $Pd(PH_3)_2$ causes distortion (the PPdP bending) with a smaller destabilization energy than $Pt(PH_3)_2$ and that the d_{HOMO} orbital of $Pd(PH_3)_2$, taking a distorted structure as in the TS, lies at relatively high energy, simialr to the d_{HOMO} orbital of $Pt(PH_3)_2$.

Introduction

Oxidative addition of the Si–X σ-bond (X = H, CH_3, SiH_3, etc.) to transition metal complexes is of central significance in syntheses of various organosilicon compounds.[1] For instance, the oxidative addition of the Si–Si σ-bond is considered to be involved as a key process in platinum- and palladium-catalyzed bis-silylation of carbon–carbon,[2–9] carbon–nitrogen,[10] and carbon–oxygen[11] multiple bonds. In this context, interesting experimental works have been reported on stoichiometric oxidative addition of the Si–X σ-bond to transition metals.[1,12–19]

Although palladium(0) complexes have often been used as catalysts in the above-mentioned bis-silylation,[1a,3–7,8c,d,9–11] a previous theoretical work revealed that the palladium(0) complex was unfavorable for the oxidative addition of H–H, C–H, and C–C bonds.[20] Thus, knowledge of the Si–X oxidative addition to the palladium(0) complex is necessary to understanding well palladium-catalyzed syntheses of organosilicon compounds. Experimentally, bis(silyl)palladium complexes have been well investigated, and several interesting results have been presented on their reductive elimination (i.e., the reverse reaction of the oxidative addition).[21,22] Besides experimental work, theoretical work is also expected to offer valid information on the Si–X oxidative addition to palladium(0) complexes.

In this work, oxidative addition of the Si–X σ-bond to $Pd(PH_3)_2$ (eq 1) is theoretically investigated with the ab initio MO/MP4 method, and compared with the same reaction of $Pt(PH_3)_2$.[23] Our aims of the present work are (1) to estimate the activation

---

[⊗] Abstract published in *Advance ACS Abstracts,* March 15, 1994.

(1) For instance: (a) Tilley, T. D. In *The Chemistry of Organic Silicon Compounds*; Patai, S., Rappoport, Z., Eds.; John Wiley & Sons: New York, 1989; p 1415. (b) Ojima, I. In *The Chemistry of Organic Silicon Compounds*; Patai, S., Rappoport, Z., Eds.; John Wiley & Sons: New York, 1989; p 1479.

(2) (a) Yamamoto, K.; Okinoshima, J.; Kumada, M. *J. Organomet. Chem.* **1971**, *27*, C31. (b) Okinoshima, H.; Yamamoto, K.; Kumada, M. *J. Organomet. Chem.* **1975**, *86*, C27. (c) Tamao, K.; Okazaki, S.; Kumada, M. *J. Organomet. Chem.* **1978**, *146*, 87.

(3) (a) Sakurai, H.; Kamiyama, Y.; Nakadaira, Y. *J. Am. Chem. Soc.* **1975**, *97*, 931. (b) Sakurai, H.; Kobayashi, T.; Nakadaira, Y. *J. Organomet. Chem.* **1978**, *162*, C43. (c) Sakurai, H.; Eriyama, Y.; Kamiyama, Y.; Nakadaira, Y. *J. Organomet. Chem.* **1984**, *264*, 229.

(4) (a) Matsumoto, H.; Shono, K.; Wada, A.; Matsubara, I.; Watanabe, H.; Nagai, Y. *J. Organomet. Chem.* **1980**, *199*, 185. (b) Watanabe, H.; Saito, M.; Sutou, N.; Nagai, Y. *J. Chem. Soc., Chem. Commun.* **1981**, 617. (c) Watanabe, H.; Saito, M.; Kishimoto, K.; Inose, J.; Nagai, Y. *J. Organomet. Chem.* **1982**, *225*, 343.

(5) Carlson, C. W.; West, R. *Organometallics* **1983**, *2*, 1801.

(6) Seyferth, D.; Goldman, E. W.; Escudié, J. *J. Organomet. Chem.* **1984**, *271*, 337.

(7) (a) Hayashi, T.; Yamamoto, A.; Iwata, T.; Ito, Y. *J. Chem. Soc., Chem. Commun.* **1987**, 398. (b) Hayashi, T.; Matsumoto, Y.; Ito, Y. *J. Am. Chem. Soc.* **1988**, *110*, 5579. (c) Murakami, M.; Andersson, P. G.; Suginome, M.; Ito, Y. *J. Am. Chem. Soc.* **1991**, *113*, 3987.

(8) (a) Hayashi, T.; Kawamoto, A. M.; Kobayashi, T.; Tanaka, M. *J. Chem. Soc., Chem. Commun.* **1990**, 563. (b) Hayashi, T.; Kobayashi, T.; Kawamoto, A. M.; Yamashita, H.; Tanaka, M. *Organometallics* **1990**, *9*, 280. (c) Yamashita, H.; Catellani, M.; Tanaka, M. *Chem. Lett.* **1991**, 241. (d) Yamashita, H.; Tanaka, M. *Chem. Lett.* **1992**, 1547.

(9) (a) Tsuji, Y.; Lago, R. M.; Tomohiro, S.; Tsuneishi, H. *Organometallics* **1992**, *11*, 2353. (b) Obora, Y.; Tsuji, Y.; Kawamura, T. *Organometallics* **1993**, *12*, 2853.

(10) (a) Ito, Y.; Nishimura, S.; Ishikawa, M. *Tetrahedron Lett.* **1987**, *28*, 1293. (b) Ito, Y.; Suginome, M.; Murakami, M. *J. Am. Chem. Soc.* **1988**, *110*, 3692.

(11) Yamashita, H.; Reddy, N. P.; Tanaka, M. *Chem. Lett.* **1993**, 315.

(12) Hoffmann, P.; Heiss, H.; Neiteler, P.; Müller, G.; Lachmann, J. *Angew. Chem., Int. Ed. Engl.* **1990**, *29*, 880.

(13) (a) Yamashita, H.; Hayashi, T.; Kobayashi, T.; Tanaka, M.; Goto, M. *J. Am. Chem. Soc.* **1988**, *110*, 4417. (b) Yamashita, H.; Kobayashi, T.; Hayashi, T.; Tanaka, M. *Chem. Lett.* **1990**, 1447. (c) Yamashita, H.; Tanaka, M.; Goto, M. *Organometallics* **1992**, *11*, 3227.

(14) Luo, X. L.; Schulte, G. K.; Demou, P.; Crabtree, R. H. *Inorg. Chem.* **1990**, *29*, 4268.

(15) Thorn, D. L.; Harlow, R. L. *Inorg. Chem.* **1990**, *29*, 2017.

(16) (a) Heyn, R. H.; Tilley, T. D. *J. Am. Chem. Soc.* **1992**, *114*, 1917. (b) Radu, N. S.; Tilley, T. D.; Rheingold, A. L. *J. Am. Chem. Soc.* **1992**, *114*, 8293.

(17) Esteruelas, M. A.; Oro, L. A.; Valero, C. *Organometallics* **1992**, *11*, 3362.

(18) Hester, D. M.; Sun, J.; Harper, A. W.; Yang, G. K. *J. Am. Chem. Soc.* **1992**, *114*, 5234.

(19) (a) Pan, Y.; Mague, J. T.; Fink, M. J. *Organometallics* **1992**, *11*, 3495. (b) Michalczyk, M. J.; Recatto, C. A.; Calabrese, J. C.; Fink, M. J. *J. Am. Chem. Soc.* **1992**, *114*, 7955.

(20) (a) Low, J. J.; Goddard, III, W. A. *J. Am. Chem. Soc.* **1986**, *108*, 6115. (b) Low, J. J.; Goddard, III, W. A. *Organometallics* **1985**, *4*, 1468.

(21) Schubert, U.; Müller, C. *J. Organomet. Chem.* **1989**, *373*, 165.

(22) Pan, Y.; Mague, J. T.; Fink, M. J. *Organometallics* **1992**, *11*, 3495.

(23) (a) Sakaki, S.; Ieki, M. *J. Am. Chem. Soc.* **1991**, *113*, 5063. (b) Sakaki, S.; Ieki, M. *J. Am. Chem. Soc.* **1993**, *115*, 2373.

0020-1669/94/1333-1660$04.50/0

$$Pd(PH_3)_2 + H_3Si\text{–}X \rightarrow cis\text{-}Pd(X)(SiH_3)(PH_3)_2 \quad (1)$$

$$X = H, CH_3, SiH_3$$

energy (E_a) and the energy of reaction (ΔE) of eq 1, (2) to show similarities and differences between $Pd(PH_3)_2$ and the Pt analogue, $Pt(PH_3)_2$, in the Si–X oxidative addition, and (3) to clarify the factors determining the reactivity of $Pd(PH_3)_2$ in this oxidative addition.

Computational Details

Ab initio MO/MP4 calculations were carried out with the Gaussian 86[24a] and 92[24b] programs. MP2 to MP4(SDQ) calculations were carried out with all the core orbitals excluded from the active space. Two kinds of basis sets, BS-I and BS-II, were mainly employed in this work; BS-I was used for geometry optimization, and BS-II was used for MP2 to MP4(SDQ) calculations. In BS-I, the 4s, 4p, 4d, 5s, and 5p orbitals of Pd were represented by a (5s 5p 4d)/[3s 3p 2d] set, where inner core electrons (up to 3d) were replaced with relativistic effective core potentials (ECPs).[25] MIDI-3 sets[26] were used for ligand atoms, except for the MINI-1 set employed for PH_3.[26,27a] In BS-II, the 4s, 4p, 4d, 5s, and 5p orbitals of Pd were represented with a (5s 5p 3d)/[3s 3p 3d] set, where inner core electrons (up to 3d) were replaced with the same ECPs as those in BS-I.[25] MIDI-4 sets[26] were used for Si, P, and C, and a (4s)/[2s] set was employed for H.[27b] In both BS-I and BS-II, the basis set of Si was augmented with a d-polarization function.[28] In BS-II, a p-polarization function[27b] was added to the basis set of H, when it directly coordinates to Pd.[29]

In the Si–Si, Si–C, and C–C oxidative additions, geometries of reactants, transition states (TS), and products were optimized with the energy gradient technique at the Hartree–Fock (HF) level, where the geometry of PH_3 was taken from the experimental structure of the free PH_3 molecule[30] and the TS was determined by calculating the Hessian matrix. In the Si–H oxidative addition, however, geometries of reactants and product were optimized at the MP2 level, using BS-I, because optimization of cis-$Pd(H)(SiH_3)(PH_3)_2$ at the HF level failed (it lead to the precursor complex, $Pd(PH_3)_2(SiH_4)$). Geometry changes during this oxidative addition were optimized at the HF level, taking the Pd–Si distance as the reaction coordinate in the early stage of the reaction, the Si–H distance in the middle stage of the reaction, and the HPdSi angle in the late stage of the reaction. The TS was roughly determined from MP4(SDQ)/BS-II calculations performed for HF-optimized geometries (see below and Figure 3 for details).

In order to ascertain the reliability of the computational method employed here, the reductive elimination (eq 2) of a model complex,

$$M(CH_3)_2 \rightarrow M + H_3C\text{–}CH_3 \quad (2)$$

$$M = Pd \text{ or } Pt$$

$M(CH_3)_2$ (M = Pd or Pt), was examined because this reaction has been investigated well with theoretical methods of high quality.[20,31] Geometries of $M(CH_3)_2$ and the TS of eq 2 were optimized with the energy gradient technique at the HF level, using BS-I. MP2 to MP4(SDQ), SD–CI, and coupled cluster calculations were carried out with BS-II and BS-III; in the latter the Huzinaga–Dunning (9s 5p)/[3s 2p] set[27b] was used for C, but the same basis sets and ECPs as those in the BS-II were adopted for Pd and H. For Pt, a (5s 5p 3d)/[3s 3p 3d] set was employed with ECPs used for core electrons (up to 4f).[25]

Table 1. Optimized Geometrical Parameters of $M(CH_3)_2$ and the TS of Reductive Elimination (M = Pd or Pt) with Bond Lengths in Å and Bond Angles in deg

		M = Pd			M = Pt	
		this work	LG[a]	SB[b]	this work	LG[a]
$M(CH_3)_2$	$R(M\text{–}CH_3)$	2.046	1.96	2.03	2.030	1.97
	∠CMC	88	92	89.9	98	98
TS	$R(M\text{–}CH_3)$	2.185	2.34	2.17	2.258	2.34
	∠CMC	58	56	58.3	50	50
	$R(C\text{–}C)$	2.133	2.14	2.114	1.969	2.14

[a] Low and Goddard.[20] Key: Pd, basis sets and ECPs of Hay et al.;[32] C, Dunning double-ζ contraction of Huzinaga's (9s 5p) primitive set;[27b] H, double-ζ contraction of Huzinaga's (4s) primitive set.[27b] [b] Siegbahn and Blomberg.[31] Key: Pd, (17s 13p 9d 3f)/[7s 6p 4d 1f];[33] C, (9s 5p)/[3s 2p];[27b] H, (5s 1p)/[3s 1p].[27c]

Table 2. Activation Energy of the Reductive Elimination of $M(CH_3)_2$ (kcal/mol)

		M = Pd		M = Pt	
		BS-II	BS-III	BS-II	BS-III
this work	HF	20.0	19.9	57.4	57.3
	MP2	20.5	20.5	57.5	56.9
	MP3	23.6	23.7	60.1	59.9
	MP4(DQ)	22.5	22.5	59.0	58.7
	MP4(SDQ)	20.5	20.4	57.1	57.0
	SD–CI(D)[a]	22.3	22.4	58.9	58.6
	SD–CI(DS)[b]	22.9	22.9	58.9	58.8
	SD–CI(P)[c]	22.7	22.7	59.1	58.7
	CCD(ST4)[d]	22.8		59.1	
LG	GVB–CI[e]	12.6[f]		53.4	
SB	CCSD(T)[g]	23.3[h]			

[a] Davidson's correction for quadratic excitations: Langhoff, S. R.; Davidson, E. R. *Int. J. Quantum Chem.* **1974**, *8*, 61. [b] Davidson and Silver's correction for quadratic excitations.[40e] [c] Pople's correction for quadratic excitations: Pople, J. A.; Seeger, R.; Krishnan, R. *Int. J. Quantum Chem., Quantum Chem. Symp.* **1977**, *11*, 149. [d] Coupled cluster (doubles) calculation with evaluation of contribution of single and triple excitations through fourth order using the CCD wave functions. [e] Low and Goddard.[20] [f] See footnote *a* of Table 1 for the basis sets used. [g] Siegbahn and Blomberg.[31] [h] See footnote *b* of Table 1 for the bsais sets used.

Results and Discussion

Prior to discussion of the Si–X oxidative addition to $Pd(PH_3)_2$, we will compare our results on the reductive elimination of $M(CH_3)_2$ (eq 2) with the results reported by Low and Goddard (LG)[20] and Siegbahn and Blomberg (SB),[31] in order to examine the reliability of our computational method employed here. In both the equilibrium structure of $M(CH_3)_2$ and the TS structure of eq 2, the $M\text{–}CH_3$ distance optimized here is similar to that reported by SB, and the optimized bond angle is almost the same as those reported by LG and SB, whereas the $M\text{–}CH_3$ distance optimized by LG slightly differs from that of SB and ours (Table 1). The activation energy (E_a) of the reductive elimination shows little dependence on the basis sets (BS-II and BS-III) and the computational methods, such as MP2 to MP4(SDQ), SD–CI, and CCD(ST4) methods (Table 2; see footnote *d* for CCD(ST4)). Our E_a value for M = Pd agrees well with the E_a value of SB,

---

(24) (a) Frisch, M. J.; Binkley, J. S.; Schlegel, H. B.; Raghavachari, K.; Melius, C. F.; Martin, R. L.; Stewart, J. J. P.; Bobrowicz, J. W.; Rohlfing, C. M.; Kahn, L. R.; DeFrees, D. J.; Seeger, R.; Whiteside, R. A.; Fox, D. J.; Fluder, E. M.; Topiol, S.; Pople, J. A. Gaussian 86. GAUSSIAN Inc., Pittsburgh, PA, 1988. (b) Frisch, M. J.; Trucks, G. W.; Gordon, M. H.; Gill, P. M. W.; Wong, M. W.; Foresman, J. B.; Johnson, B. G.; Schlegel, H. B.; Robb, M. A.; Replogle, E. S.; Gomperts, R.; Andres, J. L.; Raghavachari, K.; Binkley, J. S.; Gonzalez, C.; Martin, R. L.; Fox, D. J.; DeFrees, D. J.; Baker, J.; Stewart, J. J. P.; Pople, J. A. Gaussian 92. GAUSSIAN Inc., Pittsburgh, PA, 1992.

(25) Hay, P. J.; Wadt, W. R. *J. Chem. Phys.* **1985**, *82*, 299.

(26) Huzinaga, S.; Andzelm, J.; Klobukowski, M.; Radio-Andzelm, E.; Sakai, Y.; Tatewaki, H. *Gaussian basis sets for molecular calculations*; Elsevier: Amsterdam, 1984.

(27) (a) Van Duijneveldt, F. B. Gaussian Basis Sets for the Atoms H–Ne for Use in Molecular Calculations. *IBM J. Res. Dev.* **1971**, 945. (b) Dunning, T. H.; Hay, P. J. *Methods of Electronic Structure Theory*; Schaefer, H. F., Ed.; Plenum: New York, 1977; p 1. (c) Dunning, T. H. *J. Chem. Phys.* **1970**, *53*, 2823.

(28) Sakai, Y.; Tatewaki, H.; Huzinaga, S. *J. Comput. Chem.* **1981**, *2*, 108.

(29) When the activation energy and the energy of reaction of the Si–H oxidative addition were calculated, the p-polarization function was added to one H atom of SiH_4.

(30) Herzberg, G. *Molecular Spectra and Molecular Structure*; Academic Press: New York, 1974; Vol. 3, p 267.

(31) Siegbahn, P. E. M.; Blomberg, M. R. A. *J. Am. Chem. Soc.* **1992**, *114*, 10548.

(32) Noell, J. O.; Hay, P. J. *Inorg. Chem.* **1982**, *21*, 14.

(33) (a) Huzinaga's basis set[33b] was augmented with one diffuse d, two p, and three f functions. See ref 31 for details. (b) Huzinaga, S. *J. Chem. Phys.* **1977**, *66*, 4245.

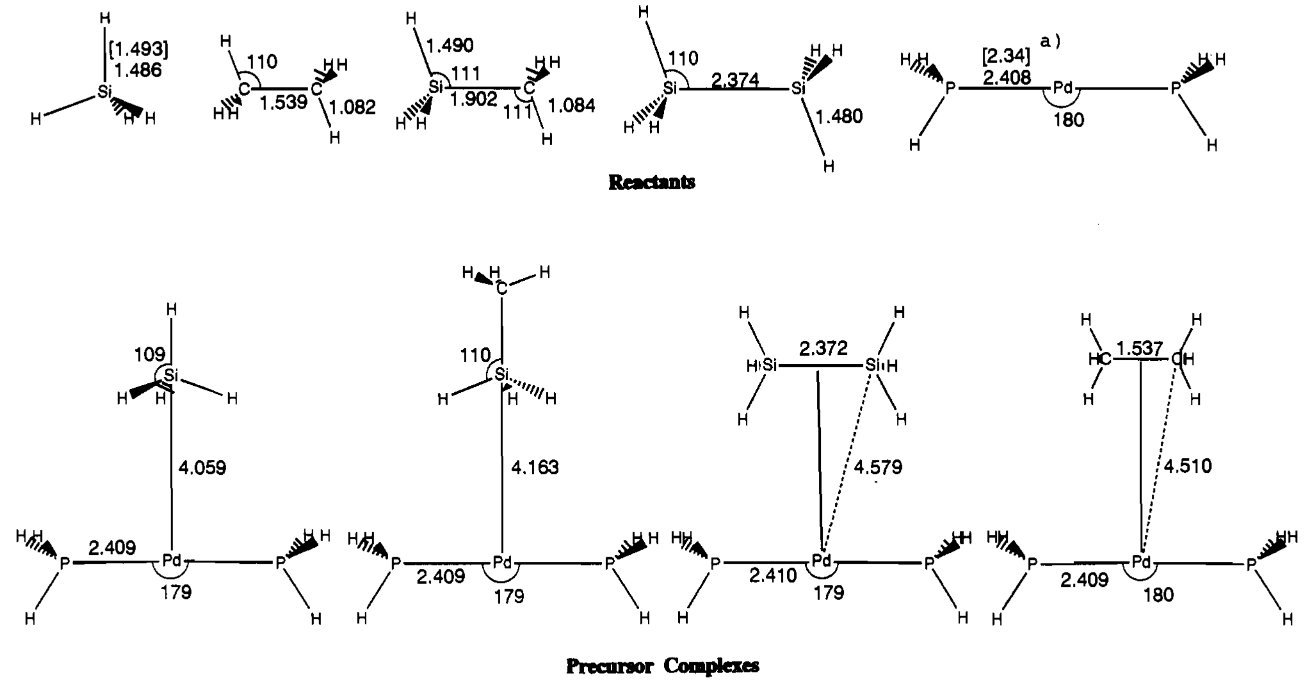

Figure 1. Optimized geometries of reactants and precursor complexes. Bond lengths are given in Å and bond angles in deg. Bond distances and bond angles which are given no value are not optimized but are assumed to be the same as in the reactants. (a) In parentheses is given the MP2/BS-I optimized value.

but is larger than the E_a value of LG by ca. 10 kcal/mol. In the case of M = Pt, our E_a value is about 5 kcal/mol larger than the E_a value reported by LG. For the purpose of comparing the Pd reaction system with the Pt system, a difference in E_a between M = Pd and M = Pt should be correctly calculated. This difference (36.6 kcal/mol), calculated here, does not differ very much from that (40.8 kcal/mol) reported by LG. All these results suggest that the MP4(SDQ)/BS-II//HF/BS-I calculation (the MP4(SDQ)/BS-II calculation of the HF/BS-I optimized structure) is reliable at least in a semiquantitative sense and in comparison of the Si–X oxidative addition to $Pd(PH_3)_2$ with the same reaction to $Pt(PH_3)_2$.

Changes in Geometry and Energy during the Si–X Oxidative Addition. Now, we will begin to consider the Si–X oxidative addition. It is often considered in this kind of oxidative addition that a substrate forms a precursor complex with a transition metal before reaching the TS.[23,34] Optimized geometries of reactants and precursor complexes are shown in Figure 1. In a precursor complex, $Pd(PH_3)_2(Si_2H_6)$, having a C_{2v}-like structure,[35a,36] the Pd–Si distance is very long (4.58 Å) and both $Pd(PH_3)_2$ and Si_2H_6 parts show little distortion (∠PPdP = 180°, *R*(Si–Si) = 2.37 Å), like the precursor complex of the Pt analogue, $Pt(PH_3)_2(Si_2H_6)$.[23] Similar features are observed in the other precursor complexes, $Pd(PH_3)_2(C_2H_6)$,[36] $Pd(PH_3)_2(SiH_4)$,[35b,36] and $Pd(PH_3)_2(SiH_3CH_3)$.[36] Consistent with these geometrical features, all the precursor complexes yield very small stabilization energies like the Pt analogues[23] (Table 3): for instance, the stabilization energy of $Pd(PH_3)_2(Si_2H_6)$ is only 3 kcal/mol (MP4(SDQ)) without the correction of basis set superposition error (BSSE) and 1.6 kcal/mol with BSSE correction.[37] These values are too small for the usual coordinate bond, indicating that these complexes can be considered as van der Waals complexes.

At the TS of the Si–Si oxidative addition (Figure 2), the Si–Si distance (2.490 Å) is 0.12 Å longer than it in the free Si_2H_6 (Figure 1), the SiH_3 group is changing its direction toward Pd, and the Pd–SiH_3 distance is still 0.4 Å longer than it is in the product, while the PPdP angle (110°) is very close to that in the product. At the TS of the Si–C oxidative addition,[38] the Pd$(PH_3)_2$ part remarkably distorts (∠PPdP = 105°), the Si–C distance lengthens by 0.33 Å, and the Pd–Si (2.450 Å) and Pd–C (2.297 Å) distances are longer than those in the product by only 0.07 and 0.18 Å respectively, suggesting that this TS is more productlike than the TS of the Si–Si oxidative addition. In the TS of the C–C oxidative addition, the PPdP angle is very small (99°) and the C–C distance is quite long (2.066 Å), about 0.53 Å longer than it in the free C_2H_6, indicating that this TS is more productlike compared to the TS of the Si–C oxidative addition. It is noted that the PPdP angles in these TSs are much smaller than those in the TSs of the Pt reaction systems; for instance, the PPdP angle is 110° and the PPtP angle is 132° for the Si–Si oxidative addition and the PPdP angle is 95° and the PPtP angle is 110° for the C–C oxidative addition, whereas Si_2H_6 and C_2H_6 parts in the TSs of Pd reaction systems are distorted to a similar extent to those in the TSs of Pt reaction systems. This interesting feature relates to the Pd d orbital energy, as will be discussed below.

---

(34) For instance: (a) Hay, P. J. *J. Am. Chem. Soc.* **1987**, *109*, 705. (b) Haynes, G. R.; Martin, R. L.; Hay, P. J. *J. Am. Chem. Soc.* **1992**, *114*, 28. (c) Daniel, C.; Koga, N.; Han, J.; Fu, X. Y.; Morokuma, K. *J. Am. Chem. Soc.* **1988**, *110*, 3773. (d) Koga, N.; Morokuma, K. *J. Phys. Chem.* **1990**, *94*, 5454.

(35) (a) The C_{2v}-like structure, in which the Si–Si bond was perpendicular to the PPdP bond, was also optimized. In this structure, both $Pd(PH_3)_2$ and Si_2H_6 parts barely distort, and the stabilization energy is almost the same as that of the C_{2v}-like structure of Figure 1. (b) The C_s-structure of $Pd(PH_3)_2(SiH_4)$ was also optimized (see Figure 2 of ref 23 for the C_s-structure), but its stabilization energy was almost the same as that of the C_{3v}-like structure (Figure 1).

(36) The structure shown in Figure 1 corresponds to the most stable structure of the Pt's precursor complex.[23] The other structures were not calculated. Even if the other structure was more stable than that in Figure 1, the energy stabilization would be absolutely small, and therefore, E_a would be little influenced, like in the Pt analogues.[23]

(37) Boys, S. F.; Bernardi, F. *Mol. Phys.* **1970**, *19*, 553. Ostlund, N. S.; Merrifield, D. L. *Chem. Phys. Lett.* **1976**, *39*, 612.

(38) (a) In optimizing this TS, the Pd–P bond distance fluctuated considerably, which made the optimization much difficult. Thus, the full optimization was abandoned, and the optimization was performed as follows: the Pd–P distances were optimized for the roughly optimized geometry[38b] of the $Pd(SiH_3CH_3)$ part, then the $Pd(SiH_3CH_3)$ part was optimized with Pd–P distances fixed, and finally, again the Pd–P distances were reoptimized. Through the reoptimization, the Pd–P distances were changed by only 0.02 Å. (b) The maximum change of geometrical parameter was ca. 0.018 Å for bond distance and ca. 2° for bond angle.

Table 3. Energy Change in Oxidative Additions[a] (kcal/mol)

	M = Pd					M = Pt[b]
	HF	MP2	MP3	MP4(DQ)	MP4(SDQ)	MP4(SDQ)
			(A) C–C Oxidative Addition			
reactants[c]	−889.0641	−889.5403	−889.5659	−889.5938	−889.6042	−881.9800
precursor	−0.2 (0.4)	−1.3 (−1.1)	−1.2 (−0.6)	−1.2 (−0.6)	−1.4 (−0.8)	−1.1 (−0.8)
TS	82.8 (85.3)	56.9 (59.3)	63.5 (65.9)	61.0 (63.5)	56.8 (59.3)	66.0 (68.5)
product	50.9	27.9	29.5	30.7	30.5	5.2
			(B) Si–Si Oxidative Addition			
reactants[c]	−1390.6068	−1391.0659	−1391.0976	−1391.1259	−1391.1380	−1383.5124
precursor	−0.6 (0.8)	−2.9 (−1.4)	−2.7 (−1.3)	−2.7 (−1.2)	−3.0 (−1.6)	−3.7 (−2.6)
TS	21.2 (24.8)	9.8 (13.4)	11.9 (15.5)	11.1 (14.7)	8.2 (11.9)	13.7 (17.0)
product	9.0	−21.1	−13.3	−16.7	−18.1	−46.4
			(C) Si–C Oxidative Addition			
reactants[c]	−1139.8416	−1140.3050	−1140.3346	−1140.3625	−1140.3740	−1132.7497
precursor	−0.6 (0.5)	−2.3 (−1.2)	−2.1 (−1.0)	−2.2 (−1.1)	−2.5 (−1.4)	−2.3 (−1.4)
TS	42.9 (46.6)	−15.1 (18.9)	22.2 (25.9)	19.2 (22.9)	16.3 (20.1)	24.9 (28.1)
product	34.0	5.9	9.9	8.7	8.1	−14.1
			(D) Si–H Oxidative Addition			
reactants[c,d]	−1100.8494	−1101.2327	−1101.2542	−1101.2809	−1101.2920	−1093.6616[e]
precursor	−2.2 (−1.2)	−1.8 (−0.8)	−2.5 (−1.5)	−2.1 (−1.1)	−2.4 (−1.4)	−6.1 (−5.8)
TS	2.6 (4.4)	−0.3 (1.5)	−0.4 (1.5)	−0.3 (1.6)	−1.3 (0.5)	−6.3 (−4.0)
product	12.5	−9.5	−4.1	−6.6	−8.1	−31.1

[a] In parentheses; basis set superposition error (BSSE) was corrected with the counterpoise method.[37] [b] Reference 23. [c] Sum of the total energies of reactants (hartree unit). [d] $Pd(PH_3)_2$ and SiH_4 were optimized at the MP2 level, using BS-I. [e] Values differ from those of ref 23, because a p-polarization function was added to H coordinating to Pt.

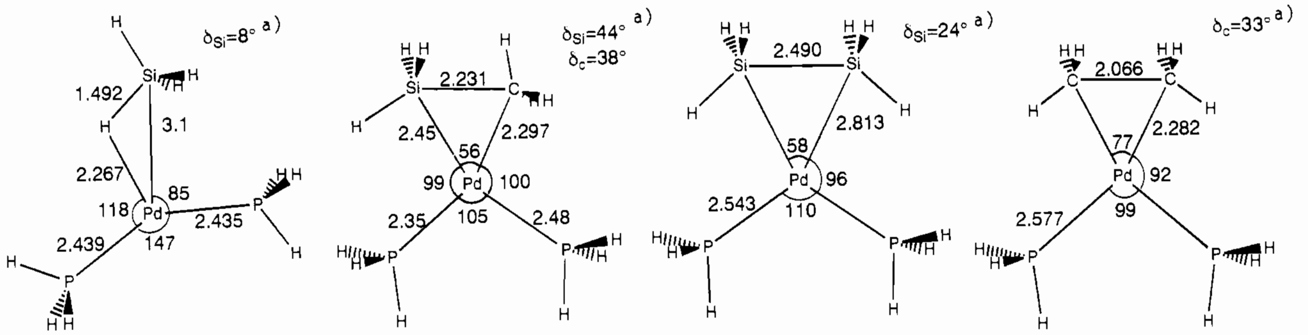

Transition States

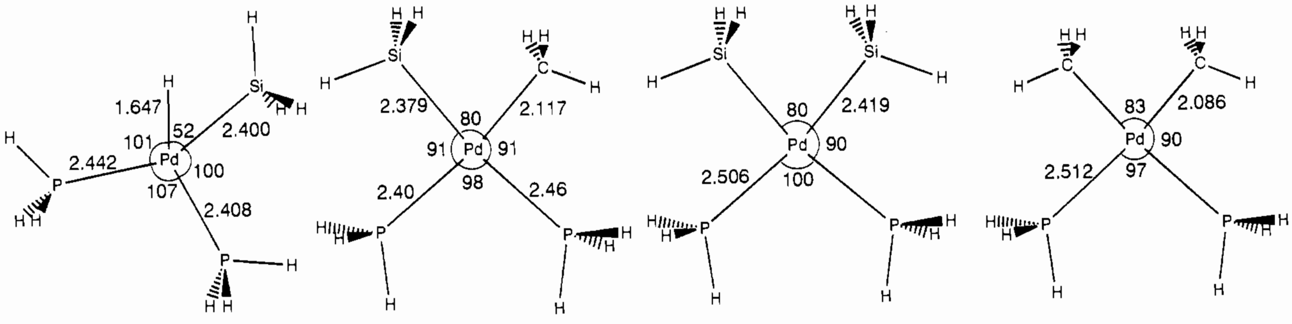

Products

Figure 2. Optimized geometries of transition states and products of the Si–X oxidative addition to $Pd(PH_3)_2$. Bond lengths are given in Å and bond angles in deg. (a) δ_x means that the XH_3 of $H_3X–YH_3$ changes its direction from Y toward Pd.

As shown in Figure 3, the Si–H oxidative addition occurs with a very small barrier at the MP4(SDQ) level. Apparently, the HF optimization of *cis*-$Pd(H)(SiH_3)(PH_3)_2$ leads to a precursor complex, $Pd(PH_3)_2(SiH_4)$, and therefore, we abandoned HF-optimization of the TS. From the MP4(SDQ)/BS-II//HF/BS-I calculations of Figure 3, the TS is roughly determined to be at around *R*(Pd–Si) = 3.1 Å. In its geometry (Figure 2), the PPdP angle is 147°, much smaller than it in the reactant, whereas the SiH_4 part distorts slightly and the Si–H distance slightly lengthens.

The activation barrier (E_a) and the energy of reaction (ΔE) of these reactions are compared in Table 3. The C–C oxidative addition to $Pd(PH_3)_2$ occurs with a quite high activation energy and a remarkably high endothermicity, as expected. The Si–Si oxidative addition, however, proceeds with a rather small activation energy and a considerable exothermicity, indicating that although the C–C oxidative addition to $Pd(PH_3)_2$ is very difficult, the Si–Si oxidative addition to $Pd(PH_3)_2$ can proceed easily. The Si–C oxidative addition is endothermic, and the

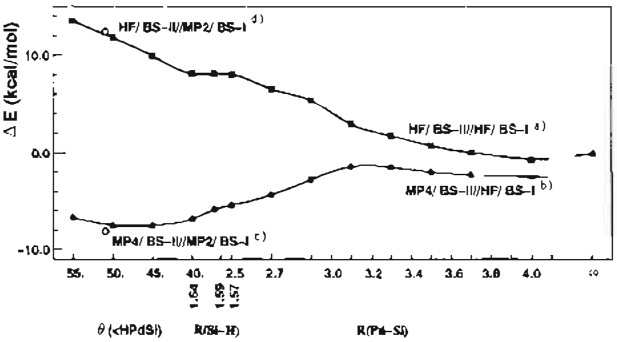

Figure 3. Energy changes during the Si–H oxidative addition to Pd$(PH_3)_2$. R(Pd–Si) and R(Si–H) are given in Å and θ is given in deg. Key: (a) HF/BS-II calculation for the geometry optimized by the HF/BS-I calculation; (b) MP4(SDQ)/BS-II calculation for the geometry optimized by the HF/BS-I calculation; (c) MP4(SDQ)/BS-II calculation for the geometry optimized by the MP2/BS-I calculation; (d) HF/BS-II calculation for the geometry optimized by the MP2/BS-I calculation.

Table 4. Estimated Pd–X and Pt–X (X = H, CH_3, or SiH_3) Bond Energies (kcal/mol)

	Pd–H	Pd–CH_3	Pd–SiH_3	Pt–H[a]	Pt–CH_3[b]	Pt–SiH_3[b]
MP2	47.0	29.5	47.0	59.9	42.2	64.4
MP3	49.1	27.7	43.3	62.2	40.2	60.3
MP4(DQ)	49.5	26.9	44.6	62.1	39.4	59.4
MP4(SDQ)	48.9	27.1	45.4	61.7	39.7	61.5

[a] Values differ from those of ref 23, because a p-polarization was added to H coordinating to Pt. [b] Reference 23.

activation energy of this reaction is much lower than that of the C–C oxidative addition but considerably higher than that of the Si–Si oxidative addition. The Si–H oxidative addition can proceed with a very small barrier (ca. 2 kcal/mol at MP4(SDQ)/BS-II) and a moderate exothermicity (8 kcal/mol at MP4(SDQ)/BS-II). In summary, the activation energy of oxidative addition to $Pd(PH_3)_2$ increases in the order Si–H < Si–Si < Si–C ≪ C–C, and the exothermicity increases in the order C–C < Si–C < Si–H < Si–Si. These orders are the same as those in the oxidative addition to $Pt(PH_3)_2$, and the reasons for this have been discussed in our previous work.[23]

Comparison between $Pd(PH_3)_2$ and $Pt(PH_3)_2$. First, let us examine the C–C oxidative addition. A significant difference between $Pd(PH_3)_2$ and $Pt(PH_3)_2$ is observed in this reaction; the C–C oxidative addition to $Pd(PH_3)_2$ is significantly endothermic, in contrast to the same reaction to $Pt(PH_3)_2$, which is only slightly endothermic (Table 3). The other Si–X oxidative addition to $Pd(PH_3)_2$ is also much less exothermic (or much more endothermic) than the corresponding reaction to $Pt(PH_3)_2$. This difference between $Pt(PH_3)_2$ and $Pd(PH_3)_2$ is easily interpreted in terms of bond energies. Bond energies are estimated at the MP2 to MP4(SDQ) levels, considering the following reactions:

$$Pd(PH_3)_2 + H_2 \rightarrow cis\text{-}Pd(H)_2(PH_3)_2 \qquad (3)$$

$$Pd(PH_3)_2 + C_2H_6 \rightarrow cis\text{-}Pd(CH_3)_2(PH_3)_2 \qquad (4)$$

$$Pd(PH_3)_2 + Si_2H_6 \rightarrow cis\text{-}Pd(SiH_3)_2(PH_3)_2 \qquad (5)$$

Apparently, as shown in Table 4, the Pd–X bond energy is smaller than the corresponding Pt–X bond energy. Thus, the oxidative addition of the Si–Si, Si–C, Si–H, and C–C bonds to $Pd(PH_3)_2$ is much less exothermic (or much more endothermic) than the corresponding reaction with $Pt(PH_3)_2$.

Interestingly, the activation energy (E_a) of the Si–X oxidative addition to $Pd(PH_3)_2$ is slightly lower than (or similar to) that of the corresponding reaction with $Pt(PH_3)_2$, whereas the former is much less exothermic (or much more endothermic) than the latter. If the bond energy was only a determining factor for the E_a value, the oxidative addition to $Pd(PH_3)_2$ would always require a considerably higher E_a value than the corresponding oxidative addition to $Pt(PH_3)_2$. Thus, the rather low E_a value indicates that the other factor is important in determining the activation barrier. At the TS, the charge-transfer from the d_{xz} orbital of $Pd(PH_3)_2$ to the σ^*-orbital of the Si–X bond is necessary to break the Si–X σ-bond (see structure I for d_{xz} and σ^*), as is well-known.[34,39] This charge-transfer interaction is, in general, considered to be weaker in the Pd atom than in the Pt atom because Pd takes a d^{10} electron configuration as its ground state but Pt takes a d^9s^1 configuration.[20] The situation, however, changes upon going to $M(PH_3)_2$ from the bare M atom (M = Pd or Pt). The d^{10} state of $Pt(PH_3)_2$ was calculated at the SD–CI level[40] to be 62 kcal/mol more stable than the $^1B_1(d^9s^1)$ state, where BS-II was used and the geometry of $Pt(PH_3)_2$ was taken to be the same as in the TS of the Si–Si oxidative addition.[23] This result suggests that the situation of the d orbital is similar in $Pd(PH_3)_2$ and $Pt(PH_3)_2$. Furthermore, $Pd(PH_3)_2$ is more flexible for PPdP bending and needs a smaller distortion energy (E_{dist}) to cause the bending than $Pt(PH_3)_2$ (note that $Pd(PH_3)_2$ is linear at the equilibrium structure but takes a bending structure at the TS, as shown in Figures 1 and 2); when the PMP angle (M = Pd or Pt) is taken to be 120°, E_{dist} = 19.1 kcal/mol for $Pt(PH_3)_2$ and 10.2 kcal/mol for $Pd(PH_3)_2$ (at the MP4(SDQ) level). This bending of $M(PH_3)_2$ pushes up the d_{xz} orbital energy. As shown by a relation between E_{dist} and the d_{xz} orbital energy (Figure 4), the d_{xz} orbital in $Pd(PH_3)_2$ rises in energy to a greater extent than it does in $Pt(PH_3)_2$, and the former lies higher in energy than the latter at the same distortion energy. The d_{xz} orbital energies ($\epsilon(d_{xz})$), the ionization potentials from the d_{xz} orbital (Ip(d_{xz})),[41] and the E_{dist} values are compared between $Pd(PH_3)_2$ and $Pt(PH_3)_2$ in Table 5, where geometries of $Pd(PH_3)_2$ and $Pt(PH_3)_2$ were taken to be the same as the distorted structures in the TS of the Si–Si oxidative addition. It is noted that although the bending (∠PPdP = 110°) of $Pd(PH_3)_2$ is much greater than that (∠PPtP = 132°) of $Pt(PH_3)_2$, the E_{dist} value of the former is slightly larger than that of the latter by only 1.7 kcal/mol (MP4-(SDQ)). Furthermore, the d_{xz} orbital in $Pd(PH_3)_2$ lies at a slightly higher energy than it does in $Pt(PH_3)_2$, and Ip(d_{xz}) is almost the same in both $Pd(PH_3)_2$ and $Pt(PH_3)_2$. All these results indicate

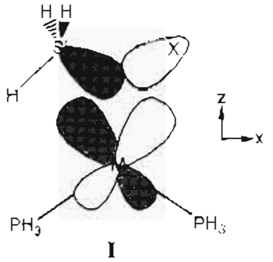

I

---

(39) For instance, Tatsumi, K.; Hoffmann, R.; Yamamoto, A.; Stille, J. K. *Bull. Chem. Soc. Jpn.* **1981**, *54*, 1857.

(40) (a) The MELD program[40b] was used for these SD–CI calculations. A single reference wave function was constructed from either HF closed shell MOs or Roothaan's restricted open-shell MOs, and the virtual orbitals were transformed to K-orbitals,[40c] where all core orbitals were excluded from the active space. To reduce numbers of excited configurations, all possible spin-adapted configuration functions were screened through the second-order Rayleigh–Schrödinger perturbation theory,[40d] and remaining excited configurations underwent variational CI calculation. The total energy from the limited SD–CI calculation was corrected by adding the correlation energy arising from the discarded excited configuration functions, and then further correction was made by estimating higher order CI expansions.[40e] (b) Davidson, E. R.; McMurchie, L.; Elbert, S.; Langhoff, S. R.; Rawlings, D.; Feller, D. MELD. University of Washington, Seattle, WA; IMS Computer Center Library, No. 030. (c) Feller, D.; Davidson, E. R. *J. Chem. Phys.* **1981**, *84*, 3997. (d) Langhoff, S. R.; Davidson, E. R. *Int. J. Quantum. Chem.* **1974**, *8*, 61. (e) Davidson, E. R.; Silver, D. W. *Chem. Phys. Lett.* **1977**, *52*, 403.

(41) Ip(d_{xz}) is calculated as an energy difference between $^1A(d^{10})$ and $^2B_1(d^9)$ states of $Pd(PH_3)_2$, where their total energies were calculated with the SD–CI method.[40]

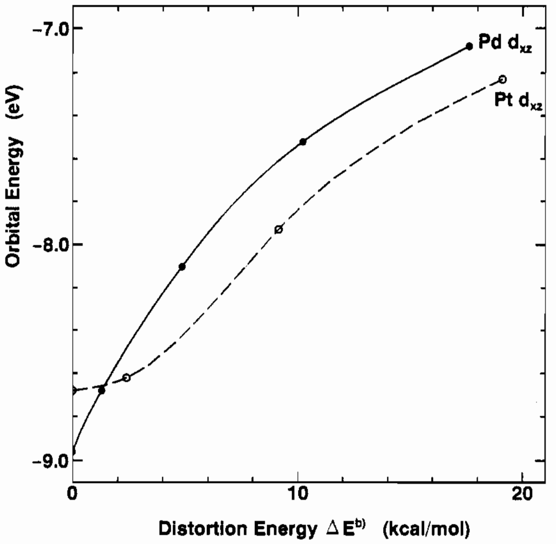

Figure 4. Relation between the d$_{xz}$ orbital energy and the bending of M(PH$_3$)$_2$ (M = Pd or Pt): (a) Only the PMP angle was changed with the M–P distance fixed to that of the equilibrium structure; (b) E_{dist} was calculated at the MP4(SDQ) level.

that Pd(PH$_3$)$_2$ can easily distort with a smaller distortion energy than Pt(PH$_3$)$_2$, and the d$_{xz}$ orbital of Pd(PH$_3$)$_2$ taking the distorted structure as in the TS lies at relatively high energy level, similar to the observation in Pt(PH$_3$)$_2$. Accordingly, a charge-transfer interaction is easily formed between the d$_{xz}$ orbital of Pd(PH$_3$)$_2$ and the Si–X σ^* orbital. Thus, the Si–X oxidative addition to Pd(PH$_3$)$_2$, as well as oxidative addition to Pt(PH$_3$)$_2$, easily occurs in spite of the low exothermicity of the former.

Table 5. Distortion Energy (E_{dist}), d$_{xz}$ Orbital Energy (ϵ(d$_{xz}$)), and Ionization Potential (Ip(d$_{xz}$))

	Pd(PH$_3$)$_2$	Pt(PH$_3$)$_2$
E_{dist}[a] (kcal/mol)	15.1	13.4
ϵ(d$_{xz}$)[b] (eV)	–7.3	–7.6
Ip(d$_{xz}$)[c] (eV)	6.0	6.2

[a] E_t(M(PH$_3$)$_2$)$_{at\ TS}$ – E_t(M(PH$_3$)$_2$)$_{eq}$ at the MP4(SDQ) level. [b] HF/BS-II calculation. [c] SD–CI/BS-II. See refs 40 and 41 for details of calculation.

Reductive Elimination from *cis*-PdX(SiH$_3$)(PH$_3$)$_2$. Finally, let us mention here the reductive elimination of *cis*-M(SiH$_3$)$_2$(PH$_3$)$_2$. The activation barrier of the reductive elimination is estimated at the MP4(SDQ) level to be 31.3 kcal/mol for M = Pd and 60.0 kcal/mol for M = Pt,[23] suggesting that the reductive elimination is much more difficult in *cis*-Pt(SiH$_3$)$_2$(PH$_3$)$_2$ but rather easy in *cis*-Pd(SiH$_3$)$_2$(PH$_3$)$_2$. The activation barrier of the Si–C reductive elimination from *cis*-Pd(SiH$_3$)(CH$_3$)(PH$_3$)$_2$ is also estimated to be 8.2 kcal/mol at the MP4(SDQ) level, showing that this reductive elimination proceeds much more easily than the Si–C reductive elimination from *cis*-Pt(SiH$_3$)(CH$_3$)(PH$_3$)$_2$ (E_a = 42.2 kcal/mol). Thus, we can expect that the palladium(0) complex is more useful as a catalyst for the reaction including both oxidative addition and reductive elimination of Si compounds than the platinum(0) complex; for instance, if the insertion of alkene and alkyne into the Pd–SiH$_3$ bond easily occurs, the palladium(0) complex is more appropriate for the bis-silylation of olefin, acetylene, butadiene, etc. than the platinum(0) complex.

Acknowledgment. A Hitachi S-820 computer at the Institute for Molecular Science (Okazaki, Japan) and an IBM-340 power station from our laboratory were used for these calculations. This work was financially supported by a grant from Ministry of Education, Culture, and Science, Japan (No. 04243102).